

CERN-TH/97-118

# Renormalization-Group Study of Weakly First-Order Phase Transitions

N. Tetradis

CERN, Theory Division,  
CH-1211, Geneva 23, Switzerland

## Abstract

We study the universal critical behavior near weakly first-order phase transitions for a three-dimensional model of two coupled scalar fields – the cubic anisotropy model. Renormalization-group techniques are employed within the formalism of the effective average action. We calculate the coarse-grained free energy and deduce the universal ratio of susceptibilities on either side of the phase transition. We compare our results with those obtained through Monte Carlo simulations and the  $\epsilon$  expansion.

PACS numbers: 05.70.Fh, 64.60.Ak, 98.80.Cq, 11.10.Wx

CERN-TH/97-118  
June 1997

A quantitative description of weakly first-order phase transitions (which are typically fluctuation driven) is necessary for a wide range of problems. Apart from their relevance to statistical systems (such as superconductors or anisotropic systems, like the one we consider below), weakly first-order phase transitions often appear in the study of high-temperature field theories. As a result they have important implications for cosmology. An example is provided by the electroweak phase transition, which is weakly first order for Higgs boson masses between approximately 40 and 80 GeV [1, 2]. The calculation of the baryon number that can be generated during the electroweak phase transition requires a precise determination of its properties.

A simple example of a system with an arbitrarily weakly first-order phase transition is the cubic anisotropy model [3, 4]. In field-theoretical language, this corresponds to a theory of two real scalar fields  $\phi_a$  ( $a = 1, 2$ ) in three dimensions, invariant under the discrete symmetry  $(1 \leftrightarrow -1, 2 \leftrightarrow -2, 1 \leftrightarrow 2)$ . It can also be considered as the effective description of the four-dimensional high-temperature theory with the same symmetry, at energy scales smaller than the temperature [5, 6]. Recently, the properties of the weakly first-order phase transitions in this model have been studied in detail, within the  $\epsilon$  expansion [7] or through Monte Carlo simulations [8]. In particular, universal amplitudes have been computed, which describe the relative discontinuity of various physical quantities along the phase transition, in the limit when the transition becomes arbitrarily weakly first order. A discrepancy has been observed in the predictions for the universal ratio of susceptibilities on either side of the phase transition obtained through Monte Carlo simulations or the  $\epsilon$  expansion [9].

In this letter we present an alternative approach that employs the exact renormalization group [10]. It is based on the effective average action  $\Gamma_k$  [11], which is a coarse-grained free energy with an infrared cutoff. More precisely,  $\Gamma_k$  incorporates the effects of all fluctuations with momenta  $q^2 > k^2$ , but not those with  $q^2 < k^2$ . In the limit  $k \rightarrow 0$ , the effective average action becomes the standard effective action (the generating functional of the 1PI Green functions), while at a high momentum scale (of the order of the ultraviolet cutoff)  $k = \Lambda \rightarrow \infty$ , it equals the classical or ‘‘microscopic’’ action. It is formulated in continuous (Euclidean) space and all symmetries of the model are preserved. The exact non-perturbative flow equation for the scale dependence of  $\Gamma_k$  takes the simple form of a renormalization-group-improved one-loop equation [12]

$$k \frac{\partial}{\partial k} \Gamma_k[\phi] = \frac{1}{2} \text{Tr} \left[ \left( \Gamma_k^{(2)}[\phi] + R_k \right)^{-1} k \frac{\partial}{\partial k} R_k \right]. \quad (1)$$

The trace involves a momentum integration and summation over internal indices. The relevant

infrared properties appear directly in the form of the exact inverse average propagator  $\Gamma_k^{(2)}$ , which is the matrix of second functional derivatives with respect to the fields. There is always only one momentum integration – multiloops are not needed – which is, for a suitable cutoff function  $R_k(q^2)$  (with  $R_k(0) \sim k^2$ ,  $R_k(q^2 \rightarrow \infty) \sim e^{-q^2/k^2}$ ), both infrared and ultraviolet finite.

The flow equation (1) is a functional differential equation, and an approximate solution requires a truncation. Our truncation is the lowest order in a systematic derivative expansion of  $\Gamma_k$  [13]

$$\Gamma_k = \int d^3x \left\{ U_k(\rho_1, \rho_2) + \frac{1}{2} Z_k \left( \partial^\mu \phi_1 \partial_\mu \phi^1 + \partial^\mu \phi_2 \partial_\mu \phi^2 \right) \right\}. \quad (2)$$

Here  $\rho_a = \frac{1}{2} \phi_a \phi^a$  and the potential  $U_k(\rho_1, \rho_2)$  is symmetric under the interchange  $1 \leftrightarrow 2$ . The wave-function renormalization is approximated by one  $k$ -dependent parameter  $Z_k$ . The truncation of the higher derivative terms in the action is expected to generate an uncertainty of the order of the anomalous dimension  $\eta$ . (For  $\eta = 0$  the kinetic term in the  $k$ -dependent inverse propagator must be exactly proportional to  $q^2$  both for  $q^2 \rightarrow 0$  and  $q^2 \rightarrow \infty$ .) For the model we are considering,  $\eta \simeq 0.035$  and the induced error is small. A similar truncation has been employed for the calculation of the equation of state for the  $O(N)$ -symmetric scalar theory [14]. The result is indeed in agreement with those obtained through alternative methods with an accuracy of order  $\eta$ .

The evolution equation for the potential results from the substitution of eq. (2) in the exact flow equation (1). The fixed-point structure of the theory is more easily identified if we use the dimensionless renormalized parameters

$$\tilde{\rho}_a = Z_k k^{-1} \rho_a \quad u_k(\tilde{\rho}_1, \tilde{\rho}_2) = k^{-3} U_k(\rho_1, \rho_2). \quad (3)$$

The evolution equation for the potential can now be written in the scale-independent form [6]

$$\frac{\partial}{\partial t} u_k(\tilde{\rho}_1, \tilde{\rho}_2) = -3u_k + (1 + \eta)(\tilde{\rho}_1 u_1 + \tilde{\rho}_2 u_2) - \frac{1}{8\pi^2} L_0^3(\tilde{m}_1^2) - \frac{1}{8\pi^2} L_0^3(\tilde{m}_2^2). \quad (4)$$

The anomalous dimension  $\eta$  is defined as  $d \ln Z_k / dt = -\eta$  and can be calculated, starting from the exact flow equation [11, 13]. For the model we are considering and the part of the phase diagram we shall study, it is constant  $\eta \simeq 0.035$  to a good approximation [6]. The quantities  $\tilde{m}_{1,2}^2$  are the eigenvalues of the rescaled mass matrix at the point  $(\tilde{\rho}_1, \tilde{\rho}_2)$

$$\tilde{m}_{1,2}^2 = \frac{1}{2} \left\{ u_1 + u_2 + 2u_{11}\tilde{\rho}_1 + 2u_{22}\tilde{\rho}_2 \pm \left[ (u_1 - u_2 + 2u_{11}\tilde{\rho}_1 - 2u_{22}\tilde{\rho}_2)^2 + 16u_{12}^2\tilde{\rho}_1\tilde{\rho}_2 \right]^{\frac{1}{2}} \right\}, \quad (5)$$

and we have introduced the notation  $u_1 = \partial u_k / \partial \tilde{\rho}_1$ ,  $u_{12} = \partial^2 u_k / \partial \tilde{\rho}_1 \partial \tilde{\rho}_2$ , etc. The function  $L_0^3(w)$ , as well as the functions  $L_1^3(w) = -dL_0^3(w)/dw$ ,  $L_{n+1}^3(w) = -1/n dL_n^3(w)/dw$  for  $n \geq 1$

that we shall encounter in the following, are negative for all values of  $w$ . Also  $|L_n^3(w)|$  are monotonically decreasing for increasing  $w$  and introduce a threshold behavior in the evolution. For large values of  $\tilde{m}_a^2$  the last two terms in eq. (4) vanish and the evolution of  $U_k$  stops. The above functions have been extensively discussed in refs. [11, 13].

The partial differential equation (4) with  $\eta = 0.035$  can be integrated numerically through a generalization of the algorithms presented in ref. [15] for the case of one background field to the case of two fields. This approach is straightforward but requires excessive computer power. An alternative solution relies on an additional approximation for the form of the potential. The expected phase structure for the theory we are considering has been discussed in detail in ref. [6] (under the assumption of a polynomial form of the potential). The phase diagram has three fixed points, which govern the dynamics of second-order phase transitions. Around one of them the system has an increased  $O(2)$  symmetry. The other two are Wilson–Fisher fixed points, corresponding to two disconnected scalar theories; they are also tricritical points separating the second-order phase transitions from two regions of first-order ones. In order to be more concrete, we consider the case where the possible minima of the potential are located on the  $\tilde{\rho}_1$  axis and concentrate on the region  $\tilde{\rho}_2 \ll 1$ . Most of the physical behavior of interest (scale-invariant form of the potential, appearance of a minimum at the origin) is observed for  $\tilde{\rho}_1 < 1$  (see fig. 1). For the above reasons we approximate the potential as

$$u_k(\tilde{\rho}_1, \tilde{\rho}_2) = v_k(\tilde{\rho}_1) + m^2 \tilde{\rho}_2 + \frac{1}{2} \lambda \tilde{\rho}_2^2 + (1+x) \lambda \tilde{\rho}_1 \tilde{\rho}_2, \quad (6)$$

with  $m^2$ ,  $\lambda$  and  $x$  constant along the  $\tilde{\rho}_1$  axis. The  $1 \leftrightarrow 2$  symmetry imposes  $m^2 = v_1(\tilde{\rho}_1 = 0)$ ,  $\lambda = v_{11}(\tilde{\rho}_1 = 0)$ . We calculate the  $k$  dependence of  $x$  from the evolution equation at  $\tilde{\rho}_1 = \tilde{\rho}_2 = 0$  [6]

$$\frac{dx}{dt} = \frac{1}{8\pi^2} (x+1)x(x-2)\lambda L_2^3(m^2). \quad (7)$$

We shall check the validity of this approximation in the following. The numerical integration of eq. (4) is now feasible, because we have only two independent variables  $(t, \tilde{\rho}_1)$  for the function  $v_k$ . The expected numerical accuracy is of order 3% [15].

We are interested in the region  $x \geq 2$ . In fig. 1 we present the evolution of  $v_1 = dv_k/d\tilde{\rho}_1$ , starting at a very high scale  $k = \Lambda$  with a “microscopic” potential  $v_\Lambda(\tilde{\rho}_1) = 1/2 \lambda_\Lambda (\tilde{\rho}_1 - \kappa_\Lambda)^2$ . All dimensionful quantities are normalized with respect to  $\Lambda$ . The initial quartic coupling is chosen arbitrarily, while the minimum  $\kappa_\Lambda$  of the “microscopic” potential is taken very close to the critical value  $\kappa_{cr}$  that separates the phase with symmetry breaking from the symmetric

one. For  $|\delta\kappa_\Lambda| = |\kappa_\Lambda - \kappa_{cr}| \ll 1$  the system spends a long “time”  $t$  of its evolution on the critical surface separating the two phases. The initial value of  $x$  is taken slightly larger than the fixed-point value 2. After the initial evolution (dotted lines) the potential settles down near the Wilson–Fisher fixed point (solid lines). The fixed point of eq. (7) at  $x = 2$  is repulsive, and  $x$  eventually evolves towards larger values. This forces the potential to move away from its scale-independent form (dashed lines). At some point in the subsequent evolution the curvature of the potential at the origin  $v_1(\tilde{\rho}_1 = 0)$  becomes positive. This signals the appearance of a new minimum there, and the presence of a fluctuation-driven first-order phase transition.

In the limit  $k \rightarrow 0$  and in the convex regions, the rescaled potential  $u_k$  grows and eventually diverges in such a way that  $U_k$  becomes asymptotically constant, equal to the effective potential  $U = U_0$ . This is apparent in fig. 2, where the potential along the  $\rho_1$  axis is plotted. The evolution of the non-convex part of the potential (between the two minima) is related to the issue of the convexity of the effective potential. This part should become flat for  $k \rightarrow 0$  [16, 17]. The approach to convexity is apparent in fig. 2, even though difficulties with the numerical integration prevent us from following the evolution all the way to  $k = 0$ . The nucleation rate during the decay of the unstable minimum can be calculated in terms of the potential at an appropriate coarse-graining scale. It is exponentially suppressed by the free energy of the dominant tunnelling configuration. The scale  $k$  must be chosen so that the pre-exponential factor, arising from fluctuations around the dominant configuration, is minimized [17]. The form of the potential during the later stages of the evolution is insensitive to the details of the “microscopic” potential. It is uniquely determined by  $\delta\kappa_\Lambda$ , and, therefore, displays universal behaviour [17].

The relative magnitude of  $|\delta\kappa_\Lambda| = |\kappa_\Lambda - \kappa_{cr}| \ll 1$  and  $\delta x_\Lambda = x_\Lambda - 2 \ll 1$  results in different types of evolution. For the type of behavior depicted in figs. 1 and 2 one must take  $|\delta\kappa_\Lambda| \ll \delta x_\Lambda$ . In the opposite limit,  $|\delta\kappa_\Lambda| \gg \delta x_\Lambda$ , the system leaves the critical surface before  $x$  evolves away from its fixed-point value. As a result, a second minimum never appears at the origin. Instead, the only minimum of the effective potential  $U_0$  is located either at zero (symmetric phase) or away from it (phase with symmetry breaking), depending on the sign of  $\delta\kappa_\Lambda$ . The resulting phase transition is second order and occurs for  $\delta\kappa_\Lambda = 0$ .

We are interested in the universal ratio of susceptibilities  $\chi_+/\chi_-$  on either side of the phase transition. This ratio depends on the value of  $|\delta\kappa_\Lambda|/\delta x_\Lambda$ . For  $|\delta\kappa_\Lambda|/\delta x_\Lambda \gg 1$  we have  $x(k) \simeq 2$  during the whole evolution. The universal quantities characterizing the second-order phase

transition are determined by the Wilson–Fisher fixed point. We calculate  $\chi_+/\chi_-$  by integrating the evolution equation and evaluating  $d^2U_0/d\phi_1^2 = \chi^{-1}$  at the minimum, for  $\delta\kappa_\Lambda = \mp\epsilon$  with  $\epsilon \ll 1$ . We obtain  $\chi_+/\chi_- = 4.0$ . This value should be compared with the value  $\chi_+/\chi_- = 4.3$ , calculated with the same method for the one-field,  $Z_2$ -symmetric theory (the Ising model) [14]. The difference is due to the approximation of the potential by eq. (6) and gives an estimate of the error induced by this assumption. The evaluation of the same quantity through the  $\epsilon$  expansion or an expansion at fixed dimension gives  $\chi_+/\chi_- = 4.8(3)$  [18]. The difference with our results is due to the truncation of eq. (2) that we have employed. Based on these comparisons we estimate a relative error of 20% in our calculation of  $\chi_+/\chi_-$ .

For  $|\delta\kappa_\Lambda|/\delta x_\Lambda \ll 1$  the potential develops a second minimum at the origin during the later stages of the evolution. The phase transition is approached by fine tuning  $\delta\kappa_\Lambda$ , so that the two minima have equal depth for  $k = 0$ . In fig. 3 we plot the difference in energy density  $\Delta U$  between the minimum away from the origin and the one at the origin, as a function of the scale  $k$ , for four values of  $\delta\kappa_\Lambda$ . The numerical integration of the evolution equation is difficult for  $k \rightarrow 0$  because of the singularity structure of  $L_n^3(w)$  [16, 17]. As a result the curves of fig. 3 must be extrapolated to  $k = 0$ . Line (a) corresponds to a system in the symmetric phase, line (d) to one in the phase with symmetry breaking. Lines (b) and (c) correspond to a system very close to the phase transition. The evolution of  $\chi_+/\chi_-$  for the same parameters is depicted in fig. 4. The extrapolated value of  $\chi_+/\chi_-$  for  $k = 0$  near the phase transition is expected to lie in the interval (1.5, 2). We have used numerical fits of various curves for  $\Delta U$  and  $\chi_+/\chi_-$  in the vicinity of the phase transition in order to perform the extrapolation to  $k = 0$ . The expected value for  $\chi_+/\chi_-$  is 1.7. We estimate an error of 0.5, resulting from the uncertainties introduced by the truncation of eq. (2), the approximation of eq. (6) and the extrapolation.

Our result  $\chi_+/\chi_- = 1.7(5)$  is depicted by a horizontal band in fig. 4. It is in good agreement with the results obtained in refs. [7, 9] through the  $\epsilon$  expansion. It disagrees with the lattice results presented in refs. [8, 9]. A value  $\chi_+/\chi_- \simeq 4$ , favored by the lattice calculation, corresponds to a theory well into the phase with symmetry breaking in our calculation (line (d) in figs. 3 and 4).

In summary, we presented a method that can provide a quantitative description of weakly first-order phase transitions. It is based on the calculation of a coarse-grained free energy through an exact flow equation. Fixed points in the evolution, the appearance of new minima in the potential, and the universal properties of the resulting fluctuation-driven first-order phase

transitions can be studied in detail. Nucleation rates can be reliably computed through an appropriate choice of the coarse-graining scale [17].

## References

- [1] K. Kajantie, M. Laine, K. Rummukainen and M. Shaposhnikov, Phys. Rev. Lett. **77**, 2887 (1996); V.A. Rubakov and M.E. Shaposhnikov, preprint CERN-TH/96-13, hep-ph/9603208; K. Jansen, preprint DESY-95-169, hep-lat/9509018.
- [2] N. Tetradis, Nucl. Phys. B **488**, 92 (1997).
- [3] J. Rudnick, Phys. Rev. B **18**, 1406 (1978).
- [4] A. Aharony, in: Phase Transitions and Critical Phenomena, vol. 6, eds. C. Domb and M.S. Green, Academic Press (1976); D.J. Amit, Field Theory, the Renormalization Group, and Critical Phenomena, World Scientific (1984).
- [5] N. Tetradis and C. Wetterich, Nucl. Phys. B **398**, 659 (1993).
- [6] S. Bornholdt, N. Tetradis and C. Wetterich, Phys. Lett. B **348**, 89 (1995); Phys. Rev. D **53**, 4552 (1996); S. Bornholdt, P. Büttner, N. Tetradis and C. Wetterich, preprint CERN-TH/96-67, cond-mat/9603129.
- [7] P. Arnold and L.G. Yaffe, preprint UW-PT-96-23, hep-ph/9610447; P. Arnold and Y. Zhang, preprint UW-PT-96-24, hep-ph/9610448.
- [8] P. Arnold and Y. Zhang, preprint UW-PT-96-26, hep-lat/9610032.
- [9] P. Arnold, S.R. Sharpe, L.G. Yaffe and Y. Zhang, Phys. Rev. Lett. **78**, 2062 (1997).
- [10] K.G. Wilson, Phys. Rev. B **4**, 3174 and 3184 (1971); K.G. Wilson and I.G. Kogut, Phys. Rep. **12**, 75 (1974); F.J. Wegner, in: Phase Transitions and Critical Phenomena, vol. 6, eds. C. Domb and M.S. Green, Academic Press (1976).
- [11] C. Wetterich, Nucl. Phys. B **352**, 529 (1991); Z. Phys. C **57**, 451 (1993); ibid. C **60**, 461 (1993); Phys. Lett. B **301**, 90 (1993).
- [12] C. Wetterich, Phys. Lett. B **301**, 90 (1993).
- [13] N. Tetradis and C. Wetterich, Nucl. Phys. B **422**, 541 (1994).

- [14] J. Berges, N. Tetradis and C. Wetterich, Phys. Rev. Lett. **77**, 873 (1996).
- [15] J. Adams, J. Berges, S. Bornholdt, F. Freire, N. Tetradis and C. Wetterich, Mod. Phys. Lett. A **10**, 2367 (1995).
- [16] A. Ringwald and C. Wetterich, Nucl. Phys. B **334**, 506 (1990); N. Tetradis and C. Wetterich, Nucl. Phys. B **383**, 197 (1992).
- [17] J. Berges and C. Wetterich, Nucl. Phys. B **487**, 675 (1997); J. Berges, N. Tetradis and C. Wetterich, Phys. Lett. B **393**, 387 (1997).
- [18] J. Zinn-Justin, Quantum Field Theory and Critical Phenomena, Oxford Science Publications (1989).

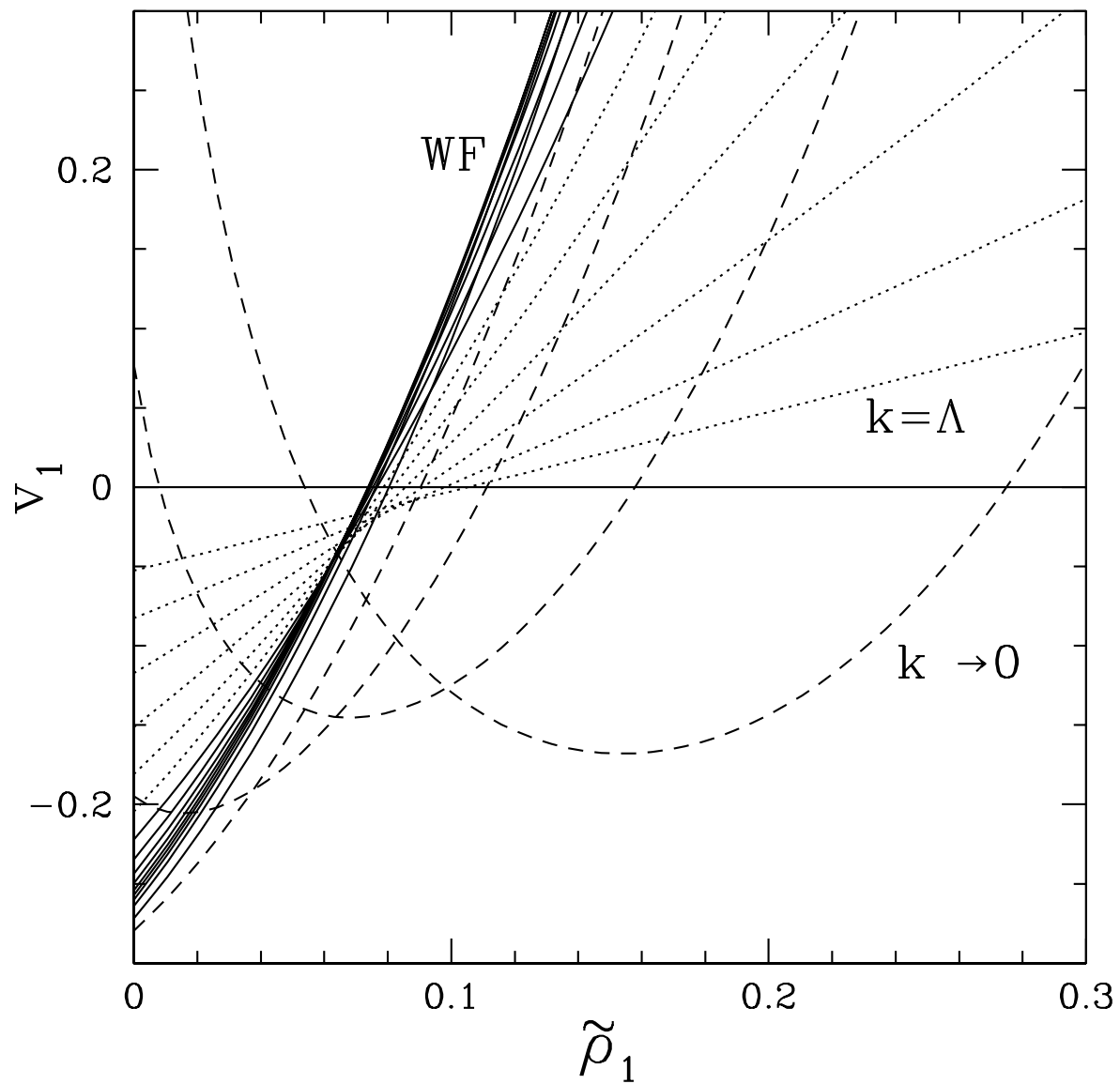


Fig. 1: The derivative of the rescaled potential along the  $\rho_1$  axis, as the coarse-graining scale is lowered.

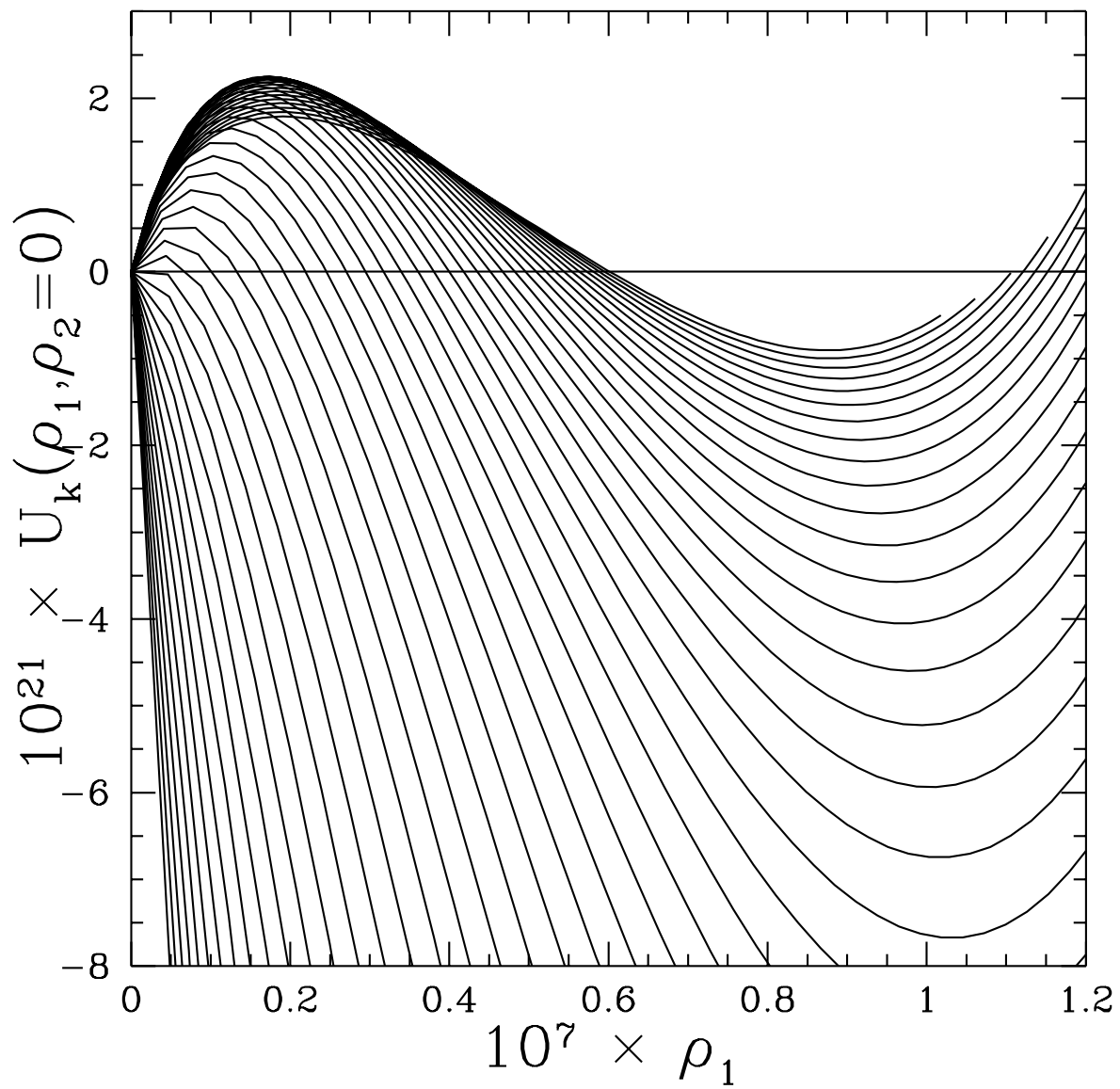


Fig. 2: The potential along the  $\rho_1$  axis, as the coarse-graining scale is lowered.

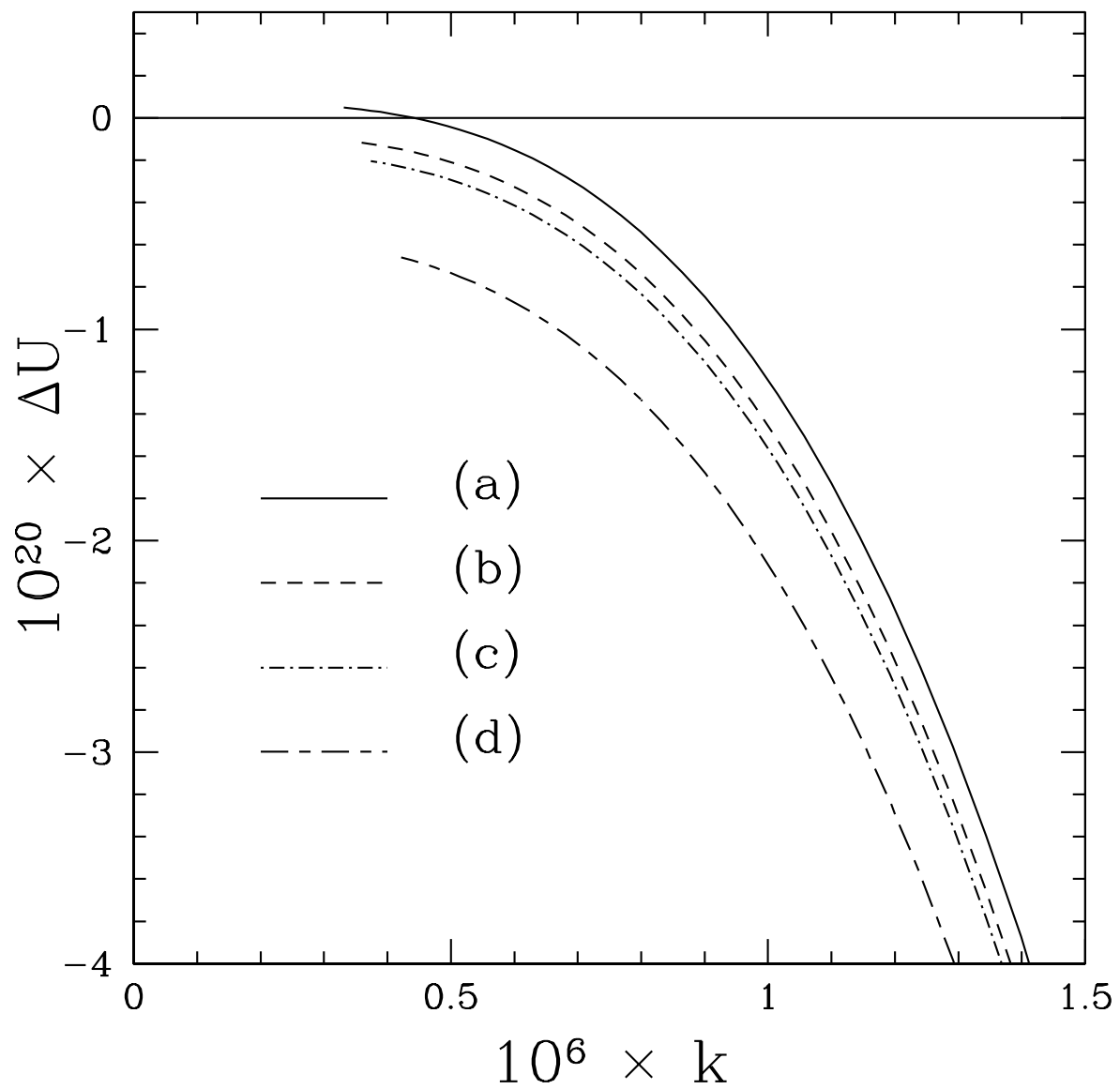


Fig. 3: The difference in energy density between the two minima of the potential, as a function of the coarse-graining scale, near the phase transition.

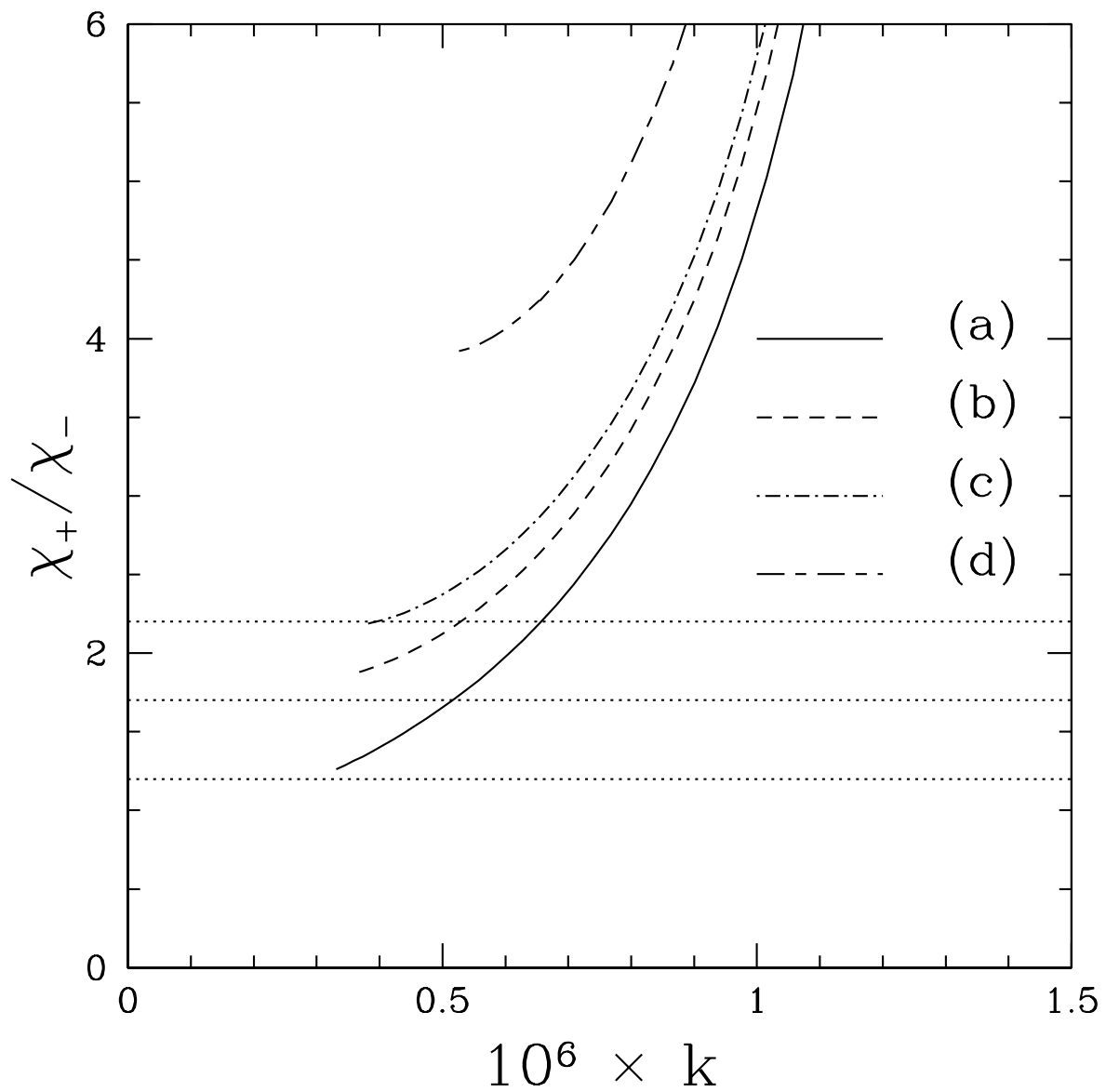


Fig. 4: The ratio of susceptibilities  $\chi_+/\chi_-$ , as a function of the coarse-graining scale, near the phase transition.